Short communication

Fabrication of micro lithium-ion battery with 3D anode and 3D cathode by using polymer wall

Kazuomi Yoshima, Hirokazu Munakata, Kiyoshi Kanamura *

Department of Applied Chemistry, Graduate School of Urban Environmental Sciences, Tokyo Metropolitan University, 1-1 Minami-Ohsawa, Hachioji, Tokyo 192-0397, Japan

ARTICLE INFO

ABSTRACT

New electrode architecture, in which a polymer wall exists in the gap between interdigitated current collectors on SiO_2/Si substrate, was developed for micro lithium-ion batteries with high power and high capacity. The polymer wall with 30 μm thickness was very helpful to construct 3D $Li_4Ti_5O_{12}$ composite anode and 3D $LiCoO_2$ composite cathode with an aspect ratio of ∼0.5, resulting in a great improvement of cell capacity up to 270 μA h cm^{-2} from 4.8 μA h cm^{-2} of the cell previously prepared by sol–gel process for $LiMn_2O_4$ cathode and $Li_4Ti_5O_{12}$ anode on a conventional non-wall electrode substrate. Furthermore, in the developed cell configuration with poly(methyl methacrylate) (PMMA) gel electrolyte, more than 60% of the discharge capacity at 2 C rate was retained at 20 C rate.

© 2012 Elsevier B.V. All rights reserved.

1. Introduction

Micro batteries have been needed for various micro devices applications. Conventionally, micro lithium-ion batteries are constructed in 2D arrangement (sandwich type structure) by thin film preparation techniques such as chemical vapor deposition (CVD) and sputtering, in which thin layers of anode, cathode, and solid electrolyte are stacked [1–10]. This configuration allows high current density with good coulomb efficiency due to fast Li$^+$ transport over a short distance between anode and cathode. Unfortunately, however, thin film lithium-ion batteries have quite a low capacity due to the dimensions of cell components, namely small amounts of active materials. Actually, both thicker anode and cathode films can be prepared with long duration of CVD or sputtering, but in that case the polarization resistance of battery greatly increases due to longer Li$^+$ transport distance between anode and cathode. Therefore, it is substantially difficult to realize both high capacity and high current density by using thin film type lithium-ion battery systems. In order to improve the cell capacity with keeping high Li$^+$ conduction, new architectures for preparation of electrodes should be developed. One of the possible electrode structures for micro batteries is a patterned electrode (Fig. 1). In our previous study, we have prepared a micro lithium-ion battery via injection processes of sols for active materials on a glass substrate with comb-type interdigitated micro current collectors [11,12]. In this electrode configuration, the Li$^+$ transport distance

between anode and cathode is kept constantly even when increasing electrode thickness. Therefore, one can simply increase the cell capacity without sacrificing rate performance. However, the use of dilute sols for active materials makes it difficult to obtain thick electrodes for practical applications. The direct deposition of active material particles onto target current collectors can be performed by using their suspensions, but it is also difficult to fabricate 3D electrode with high aspect ratio due to overlapped deposition of anode and cathode materials [13]. The concept and advantages of 3D electrode configuration has been thoroughly reviewed by Long et al. [14]. In fact, some of 3D electrodes were developed by using micromachining and templating techniques [15–17]. However, 3D batteries have not been practically realized due to difficulty in the assembly of 3D anode and 3D cathode.

So far, we have been focusing on new electrode architecture for increasing the capacity of micro lithium-ion batteries, in which a wall structure of polymer is formed between the interdigitated current collectors. In the previous work, we preliminarily confirmed that the polymer wall works as the support to prepare 3D anode and cathode with higher aspect ratios, and successfully obtained 3D $LiFePO_4$ composite cathode and Sn–Ni alloy anode [18]. The prepared 3D electrodes resulted in a great improvement of cell capacity up to 114.9 μA h cm^{-2} from 4.8 μA h cm^{-2} of the cell prepared with a conventional non-walled electrode substrate. However, the performance of cell with this 3D configuration could not be adequately evaluated owing to the poor cycleability and low rate capability of Sn–Ni alloy anode. Therefore in this study, conventional $LiCoO_2$ and $Li_4Ti_5O_{12}$ were used to prepare 3D micro lithium-ion battery and the effect of 3D electrode configuration on cell performance was thoroughly evaluated, particularly focusing on the rate capability.

* Corresponding author. Tel.: +81 42 677 2828; fax: +81 42 677 2828.
E-mail address: kanamura@tmu.ac.jp (K. Kanamura).
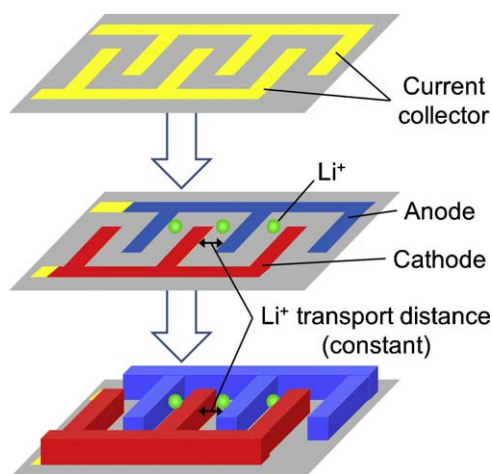
Fig. 1. The concept of electrode design for increasing cell capacity with keeping good rate performance in micro lithium-ion batteries.

2. Experimental

A flat SiO$_2$/Si substrate, on which interdigitated current gold collectors with the support polymer wall between them were formed, was supplied from Tokyo Ohka Kogyo Co., Ltd. and used as-received. The width of current collectors and polymer wall was 20 μm. The thickness of polymer wall was 30 μm. Li$_4$Ti$_5$O$_{12}$ and LiCoO$_2$ were used as anode and cathode materials, respectively. Commercially available Li$_4$Ti$_5$O$_{12}$ with ~10 μm particle size was ball-milled for 12 h to obtain its small particles with an average diameter of 100 nm. The prepared Li$_4$Ti$_5$O$_{12}$ powder was mixed with acetylene black, carboxymethylcellulose, styrene–butadiene rubber in a weight ratio of 91.1:6.5:1.0:1.4, and then dispersed in Milli-Q water (Milli-Q gradient A10, Millipore) to prepare the slurry for anode. Similarly, the cathode slurry was prepared with LiCoO$_2$, which is commercially available with an average particle size of 5 μm. 3D anode and 3D cathode were selectively formed on the interdigitated current collectors by casting the slurries by using a micro-injection system (Injectman NI2, Eppendorf) with a glass capillary with 10 μm inner diameter under an optical microscope observation (BX51W1, Olympus). After the injection process, the electrode substrate was dried at 85 °C in vacuum for 12 h, and then immersed in acetone for several seconds to remove the polymer wall. In this study, poly(methyl methacrylate) (PMMA) gel electrolyte, which has ionic conductivity of ca. 1×10^{-3} S cm^{-1} at 25 °C, was used to construct 3D micro lithium-ion battery. The PMMA gel electrolyte was prepared by thermal polymerization of methyl methacrylate (MMA) in ethylene carbonate/diethyl carbonate (1/1, v/v) containing 1 mol dm^{-3} LiClO$_4$ (EC/DEC-LiClO$_4$) at 80 °C for 1 h under Ar atmosphere [19]. Ethylene glycol dimethacrylate (EGMA) and azobisisobutyronitrile (AIBN) were used as a cross-linking agent and a polymerization initiator, respectively. All the reagents, except of EC/DEC-LiClO$_4$ (Kishida Chemical), were purchased from Wako Pure Chemical Industries. The precursor solution of PMMA gel electrolyte with the weight ratio of MMA:EGMA:AIBN:EC/DEC-LiClO$_4$ = 1:0.05:0.02:2.87 was filled into the vacancies of anode and cathode as well as their gap up to ~500 μm thickness, and then thermally polymerized to prepare 3D micro lithium-ion battery.

The formation of 3D anode and cathode was confirmed with an optical microscope and a scanning electron microscope (SEM, JSM-6490A, JEOL) equipped with an energy dispersive X-ray (EDX) spectrometer. Cyclic voltammetry (CV) was carried out using a potentiostat (HSV-100, Hokuto Denko) in the potential rage of 1.5–2.5 V at a scan rate of 10 mV min^{-1}. The charge and discharge behaviors were measured using ALS760B (BAS) at different charge and discharges rates from 2 C to 20 C. The cut-off voltages for the discharge and charge processes were set to 1.5 and 2.5 V, respectively. All the electrochemical measurements were performed at 25 °C under Ar atmosphere.

3. Results and discussion

Fig. 2 shows typical SEM images of the electrode substrate. It was clearly found that a polymer wall with 30 μm thickness existed in each gap between interdigitated current collectors. During the injection of electrode slurry into the space on the target current collector, the polymer wall was settled stably. Fig. 3 shows surface and cross-sectional SEM images of the Li$_4$Ti$_5$O$_{12}$ anode and LiCoO$_2$ cathode formed on the electrode substrate. After the elimination of polymer wall by immersion of the electrode substrate in acetone, the dimensions of anode and cathode were successfully maintained. Both electrodes have a thickness of ~15 μm. This result shows that the polymer wall effectively worked as a support to prepare 3D electrodes. The smaller thicknesses of anode and cathode compared with 30 μm of the polymer wall were due to the volume shrinkage by drying the slurries. From the EDX mapping images (Fig. 4), it is confirmed that Co and Ti elements distributed
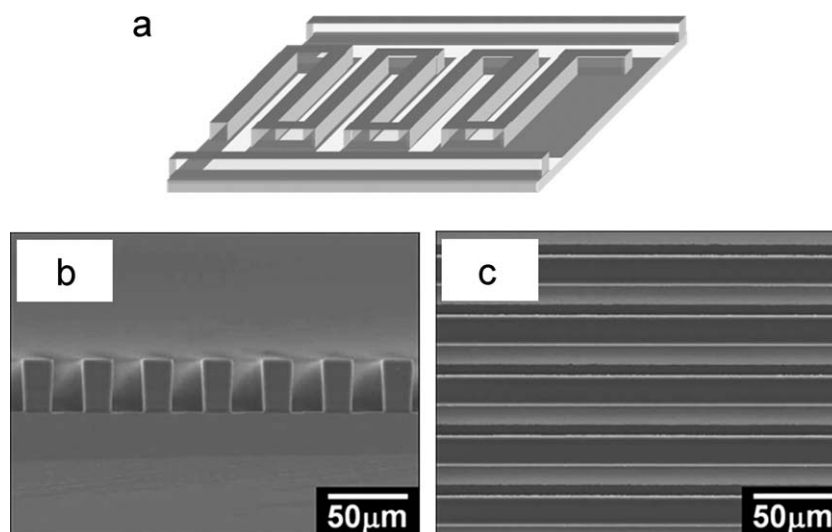
Fig. 2. (a) Schematic illustration of the electrode substrate used in this study and its (b) surface and (c) cross-sectional SEM images.
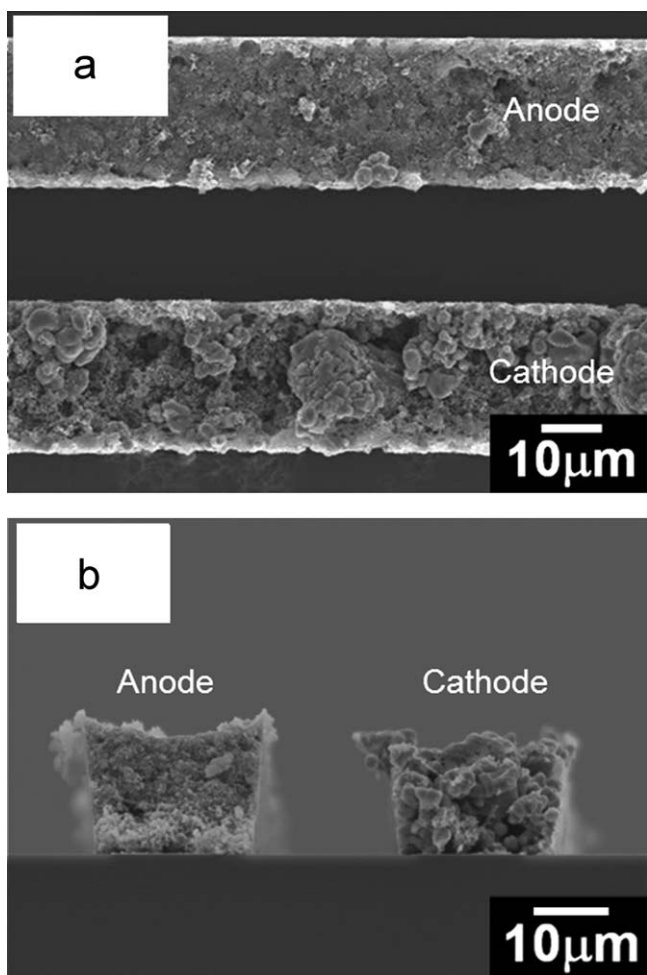
Fig. 3. (a) Surface and (b) cross-sectional SEM images of 3D $Li_4Ti_5O_{12}$ composite anode and 3D $LiCoO_2$ composite cathode fabricated on the electrode substrate.

Fig. 4. EDX mapping image of 3D $Li_4Ti_5O_{12}$ composite anode and 3D $LiCoO_2$ composite cathode fabricated on the electrode substrate, corresponding to Fig. 3(b).

Fig. 5. Cyclic voltammogram of the 3D micro lithium-ion battery with $Li_4Ti_5O_{12}$/PMMA-gel/$LiCoO_2$ configuration, obtained at a scan rate of $10\,mV\,min^{-1}$.

Fig. 6. Charge and discharge curves of the 3D micro lithium-ion battery obtained at various rates (upper and lower cut-off voltages: 2.5 and 1.5 V).

selectively with 3D configuration. This result also suggests the selective formation of anode and cathode on interdigitated current collectors. It is noticeable that the $LiCoO_2$ cathode was more porous than the $Li_4Ti_5O_{12}$ anode. This difference is due to the larger particle size and wider size distribution of $LiCoO_2$ than $Li_4Ti_5O_{12}$.

Fig. 5 shows the cyclic voltammogram of the 3D micro lithium-ion battery with $Li_4Ti_5O_{12}$/PMMA-gel/$LiCoO_2$ configuration. A couple of anodic and cathodic peaks were observed at around 2.35 V, which corresponds to the cell voltage of Li^+ insertion/extraction expected from the redox potentials of $Co^{3+/4+}$ in $LiCoO_2$ and $Ti^{4+/3+}$ in $Li_4Ti_5O_{12}$. This electrochemical behavior is in good agreement with the results reported previously [10,20–22].

Fig. 6 shows the charge and discharge curves of the 3D micro lithium-ion battery, obtained at different charge and discharge rates. The cell successfully operated with a potential plateaus at ~2.35 V in both charging and discharging processes. This potential agrees with that estimated from the cyclic voltammogram shown in Fig. 5. The discharge capacity was estimated to be $270\,\mu A\,h\,cm^{-2}$ at 2 C rate ($0.42\,mA\,cm^{-2}$), which is normalized against the total surface area of anode and cathode current collectors. This capacity is extremely high compared with those reported for micro batteries with conventional thin-film configurations [23]. The utilization of active materials is estimated to be 77% based on the amount of deposited $Li_4Ti_5O_{12}$ and $LiCoO_2$ and their theoretical capacities. It is noteworthy that the cell operates reversibly and shows about $170\,\mu A\,h\,cm^{-2}$ even at 20 C rate, although the polarization becomes gradually larger as increasing charging and discharging rates. Fig. 7
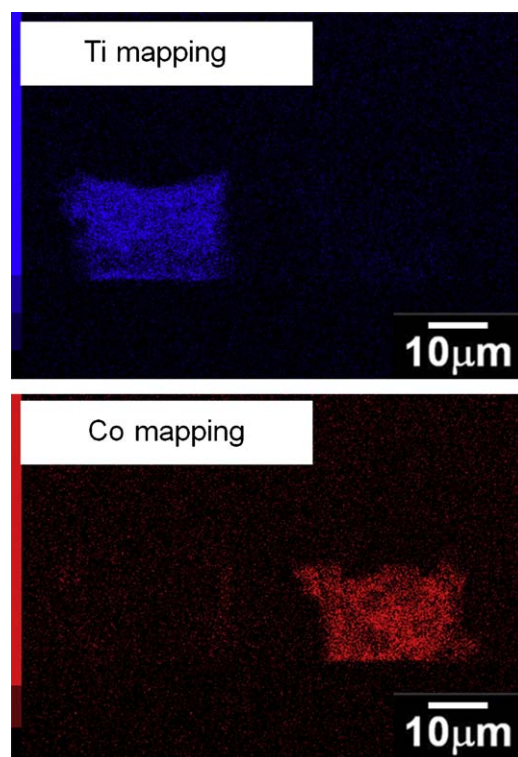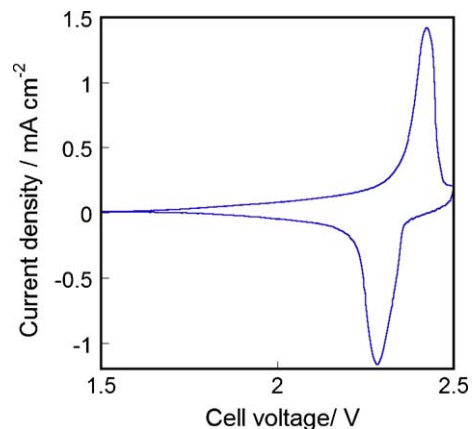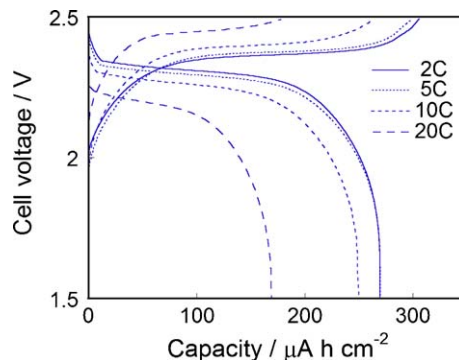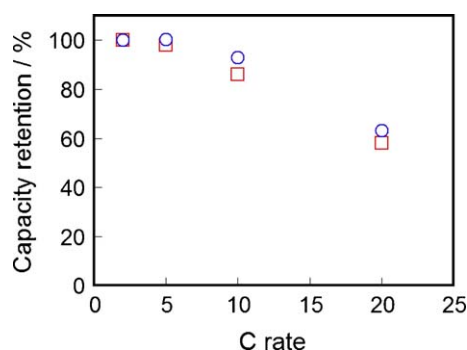
Fig. 7. Capacity retention of the 3D micro lithium-ion battery at various rates, calculated as a relative value against the specific capacity obtained at 2 C rate (charge capacity, □; discharge capacity, ○).

shows the capacity retention of the 3D micro lithium-ion battery. Each plotted point is a relative value against the specific capacity obtained at 2 C rate. In the case of composite electrodes/PMMA-gel system with conventional electrode configuration, the capacity retention is about 50% when the discharge rate changes from 0.1 C to 2 C [24]. On the contrary, the 3D micro lithium-ion battery showed excellent rate capability. In the case of discharging at 20 C rate, the capacity retention was 63%. As mentioned above, the diffusion length of Li^+ between anode and cathode can be maintained constantly in the electrode configuration developed in this study even when the electrode thickness increases. The gap between anode and cathode in the prepared cell was 20 μm, which enabled the fast Li^+ transfer between the electrodes even when PMMA-gel was used as the electrolyte. To the best of our knowledge, it is the best performance to realize both high capacity and good rate capability in micro lithium-ion batteries. The diffusion rate of Li^+ is proportional to the square of the distance that Li^+ travels. Therefore, the rate capability of cell with 3D electrode configuration can be further improved as decreasing gap between anode and cathode. Recently, we have succeeded to prepare the substrate with 10 μm electrode gap.

Fig. 8 shows the cycle performance of the 3D micro lithium-ion battery. Both charge and discharge were performed at 2 C rate after the rate capability test shown in Fig. 6. A good reversibility was confirmed although a small capacity fading was observed. This small capacity fading is considered to be due to the electrochemical property of the ball-milled $Li_4Ti_5O_{12}$ powder used for anode. It has been reported by Hong et al. that the cycleability of active materials changes according to ball-milling conditions [25]. Actually, the as-purchased $Li_4Ti_5O_{12}$ showed good cycleability with $\sim$160 mA h g^{-1} in the half cell test using 2032 coin-type cell. However, its cycleability became poor and the specific

capacity decreased to $\sim$135 mA h g^{-1} after the ball-milling for 12 h. Therefore, the performance of 3D micro lithium-ion battery is expected to be improved by optimizing the ball-milling condition of $Li_4Ti_5O_{12}$. Of course, the use of small particles of $Li_4Ti_5O_{12}$ with good cycleability or other active materials with higher specific capacity such as $LiNi_{1/3}Mn_{1/3}Co_{1/3}O_2$ and Li_2MnO_3–$LiMO_2$ (M: Ni, Co, Mn) is one of effective approaches to improve the cell performance.

4. Conclusions

The fabrication of micro lithium-ion battery with 3D anode and 3D cathode was demonstrated by using an electrode substrate with 30 μm polymer wall on the gap between interdigitated current collectors. The polymer wall effectively worked as the support and provided 3D $Li_4Ti_5O_{12}$ composite anode and 3D $LiCoO_2$ composite cathode with an aspect ratio of $\sim$0.5. The 3D micro lithium-ion battery with $Li_4Ti_5O_{12}$/PMMA-gel/$LiCoO_2$ configuration operated reversibly at 2.35 V with the discharge capacity of 270 μA h cm^{-2} at 2 C rate. Although the capacity gradually decreased as increasing rates of charging and discharging, more than 60% of retention was realized even at 20 C rate. This result clearly showed the superiority of 3D electrode configuration for co-achieving high capacity and good rate capability. The fabrication processes for 3D micro lithium-ion battery is still under optimization. Particularly, the contact between a composite electrode and a current collector should be improved. A composite electrode is generally pressed to a current collector to improve their contact. However, the pressing process was excluded in this study due to handling difficulty. The demands for 3D design of electrodes are recently increasing not only in the field of lithium-ion batteries but also in another energy conversion devices such as fuel cells and solar cells. The method developed in this study also has many possibilities to meet such upcoming demands.
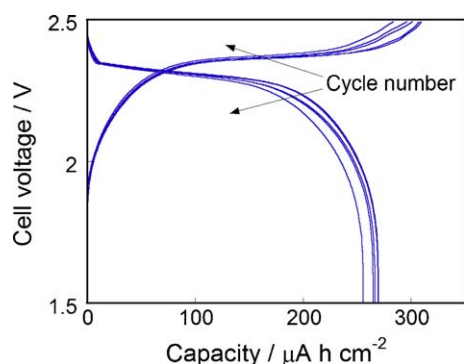
Fig. 8. Cycle performance of the 3D micro lithium-ion battery at 2 C rate, after the rate capability test (upper and lower cut-off voltages: 2.5 and 1.5 V).

References

[1] J. Song, X. Yang, S.S. Zeng, M.Z. Cai, L.T. Zhang, Q.F. Dong, M.S. Zheng, S.T. Wu, Q.H. Wu, J. Micromech. Microeng. 19 (2009) 045004.
[2] H. Mazor, D. Golodnitsky, L. Burstein, E. Peled, Electrochem. Solid-State Lett. 12 (2009) A232–A235.
[3] J.B. Bates, N.J. Dudney, D.C. Lubben, G.R. Gruzalski, B.S. Kwak, X. Yu, R.A. Zuhr, J. Power Sources 54 (1995) 58–62.
[4] H. Porthault, F. Le Cras, S. Franger, J. Power Sources 195 (2010) 6262–6267.
[5] J. Deng, Z. Lu, I. Belharouak, K. Aminem, C.Y. Chung, J. Power Sources 193 (2009) 816–821.
[6] Y. Yu, J.L. Shui, C.H. Chen, Solid-State Commun. 135 (2005) 485–489.
[7] V. Patil, A. Patil, J.W. Choi, Y.P. Lee, Y.S. Yoon, H.J. Kim, S.J. Yoon, J. Electroceram. 23 (2009) 214–218.
[8] Y. Zhao, G. Liu, L. Liu, Z. Jiang, J. Solid State Electrochem. 13 (2011) 705–711.
[9] V. Patil, A. Patil, J.W. Choi, S.J. Yoon, Solid State Sci. 13 (2011) 1232–1234.
[10] J. Song, S. Jacke, D. Becker, R. Hausbrand, W. Jaegermann, Electrochem. Solid-State Lett. 14 (2011) A11–A13.
[11] K. Dokko, J. Sugaya, H. Nakano, T. Yasukawa, T. Matsue, K. Kanamura, Electrochem. Commun. 9 (2007) 857–862.
[12] H. Nakano, K. Dokko, J. Sugaya, T. Yasukawa, T. Matsue, K. Kanamura, Electrochem. Commun. 9 (2007) 2013–2017.
[13] M. Hirokazu, T. Sugiura, K. Kanamura, Fanc. Mater. Lett. 2 (2009) 9–12.
[14] J.W. Long, B. Dunn, D.R. Rolison, H.S. White, Chem. Rev. 104 (2004) 4463–4492.
[15] M. Beidaghi, C. Wang, Electrochem. Acta 56 (2011) 9508–9514.
[16] C. Lethien, M. Zegaoui, P. Roussel, P. Tilmant, N. Rolland, P.A. Rolland, Microelectron. Eng. 88 (2011) 3172–3177.
[17] C. Wang, L. Taherabadi, G. Jia, M. Madou, Y. Yeh, B. Dunn, Electrochem. Solid-State Lett. 7 (2004) A435–A438.

[18] H. Munakata, K. Yoshima, K. Kanamura, IOP Conf. Ser.: Mater. Sci. Eng. 18 (2011) 122007.
[19] S. Kuwabata, M. Tomiyori, J. Electrochem. Soc. 149 (2002) A988.
[20] M. Hirayama, K. Kim, T. Toujigamori, W. Cho, R. Kanno, Dalton Trans. 40 (2011) 2882–2887.
[21] K. Kanamura, T. Chiba, K. Dokko, J. Eur. Ceram. Soc. 26 (2006) 577–581.
[22] M.M. Thackeray, J. Electrochem. Soc. 141 (1994) L147–L150.
[23] X. Zhu, Z. Guo, G. Du, P. Zhang, H. Liu, Surf. Coat. Technol. 204 (2010) 1710–1714.
[24] D.W. Kim, J. Power Sources 87 (2000) 78–83.
[25] C.H. Hong, A. Noviyanto, J.H. Ryu, J. Kim, D.H. Yoon, Ceram. Int. 38 (2012) 301–310.